Silencing of preBötzinger Complex somatostatin–expressing neurons induces persistent apnea in awake rats

Wenbin Tan[1]*, Wiktor A. Janczewski[1]*, Paul Yang[1], Xuesi M. Shao[1], Edward M. Callaway[2], and Jack L. Feldman[1#]

[1]Department of Neurobiology, Box 951763, David Geffen School of Medicine at University of California, Los Angeles, 650 Charles Young Dr. South, Los Angeles, CA 90095, USA

[2]System Neurobiology Laboratories, The Salk Institute for Biology Studies, 10010 North Torrey Pines Road, La Jolla, CA 92037, USA

[*]These authors contributed equally to this work.

[#]To whom correspondence should be addressed: E–mail: feldman@ucla.edu

Supplementary Figures

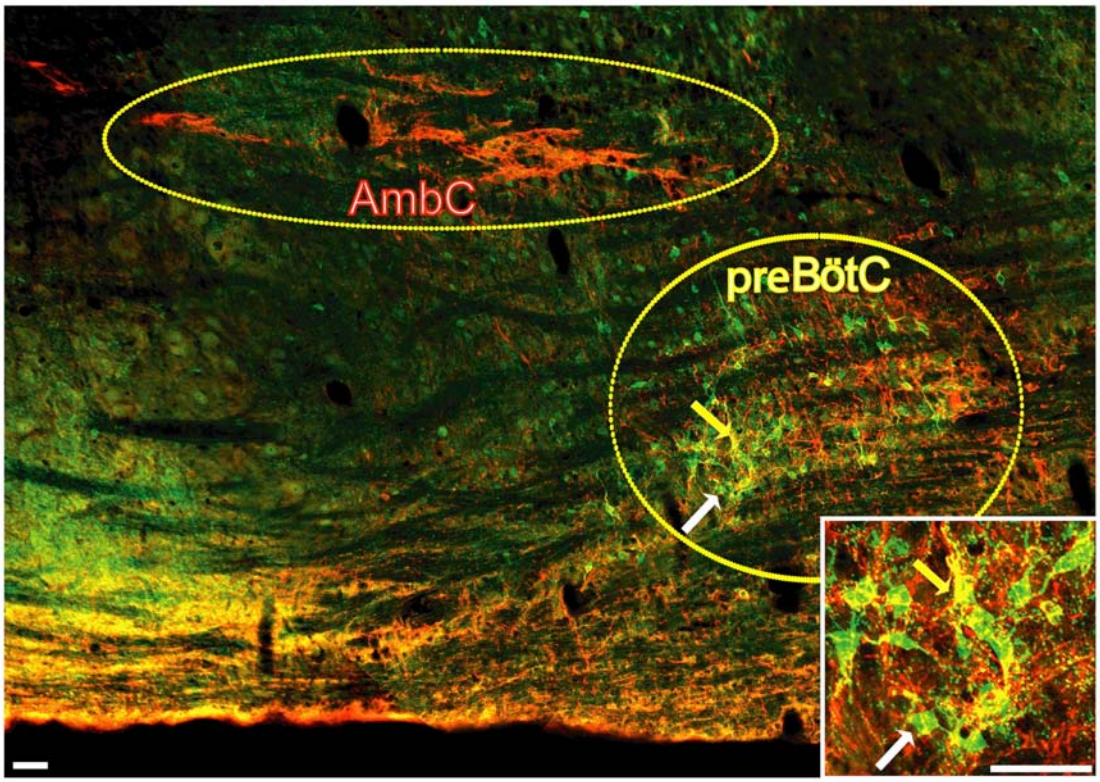

Supplementary Figure 1 Sst neurons partially overlap with NK1R neurons in preBötC in young adult (5-6 weeks) rats**.** Double-labeling with appropriate antibodies show NK1R-ir (red) and Sst-ir (green) neurons in sagittal section. Inset is high magnification of indicated neurons. Yellow arrow indicates neuron with colocalization of NK1R-ir and Sst-ir, whereas white arrow represents Sst-ir only. AmbC: ambiguus nucleus compact; scale bar, 50 μm.

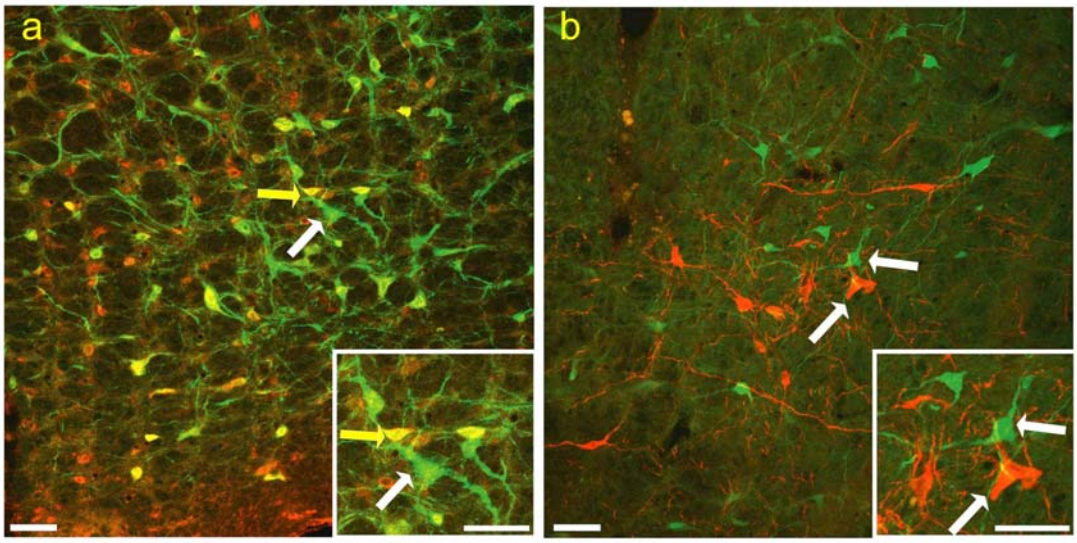

Supplementary Figure 2 Characterization of preBötC neurons infected by AAV2-Syn-AlstR-EGFP. (**a**) Double-labeling showing EGFP-ir (green) and Sst-ir (red) neurons; (**b**) Double-labeling showing EGFP (green) and tyrosine hydroxylase-ir (TH, red) neurons. All images were obtained by confocal microscopy. Insets are high magnification of indicated neurons. Yellow arrows represent neurons coexpressing relevant markers; white arrows represent neurons not coexpressing. Scale bar, 50 μm.

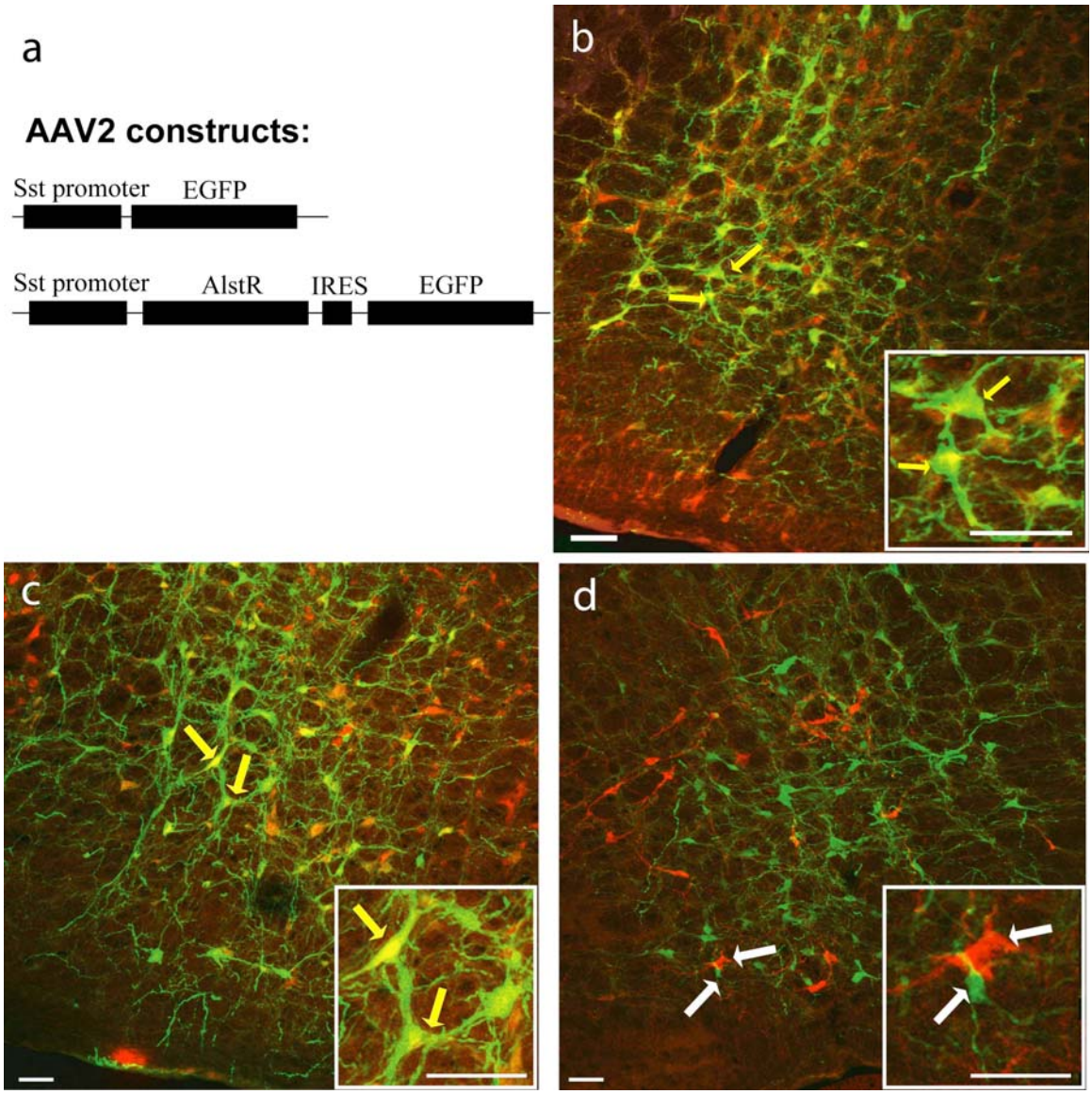

Supplementary Figure 3 Characterization of preBötC neurons infected by AAV2 containing the Sst promoter. (**a**) Schematic representation of AAV2 viral vectors with Sst promoter. (**b**) Sst-AlstR-EGFP AAV2 specifically targeted preBötC Sst neurons. EGFP-ir (green) and SST-ir (red). (**c**) Sst-AlstR-EGFP infected cells are preBötC neurons. Double staining with NeuN-ir (red) and EGFP-ir (green). (**d**) Sst-AlstR-EGFP did not infect TH-ir neurons. Double staining with TH-ir (red) and EGFP-ir (green). All images were obtained by confocal microscopy. Insets are high magnification of indicated neurons. Yellow arrows represent neurons coexpressing relevant markers; white arrows represent neurons not coexpressing. Scale bar, 50 μm.

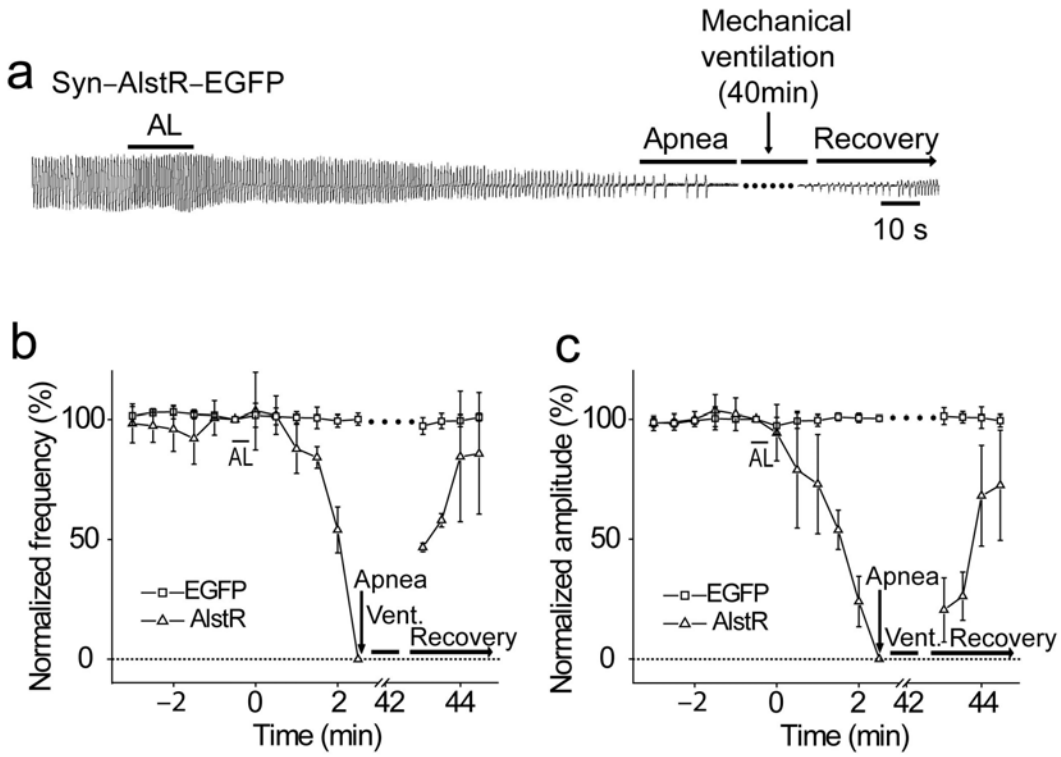

Supplementary Figure 4 Rapid silencing of preBötC AlstR-expressing neurons induces apnea in anesthetized rats. AL was administered (0.42 μmole kg^{-1}, intracerebellomedullary cisternally (*icc*)) 4-6 weeks after bilateral preBötC microinjection of Syn-AlstR-EGFP. (**a**) Changes of breathing pattern of anesthetized rat upon AL application; mechanical ventilation for duration of apnea (~40 min). (Signal represents respiratory airflow). (**b**)**,** (**c**)**,** AL administration induced a gradual decline of both frequency (b) and tidal volume (c) until apnea developed at 2.5 min post-AL application. After mechanical ventilation, the rats resumed spontaneous breathing. Vent., ventilation; Values are group mean±s.d. (n=5). Note: in n=3 out of 5 rats, there was a significant increase in ventilation ~20 sec after administration of AL (Supplementary Fig 5).

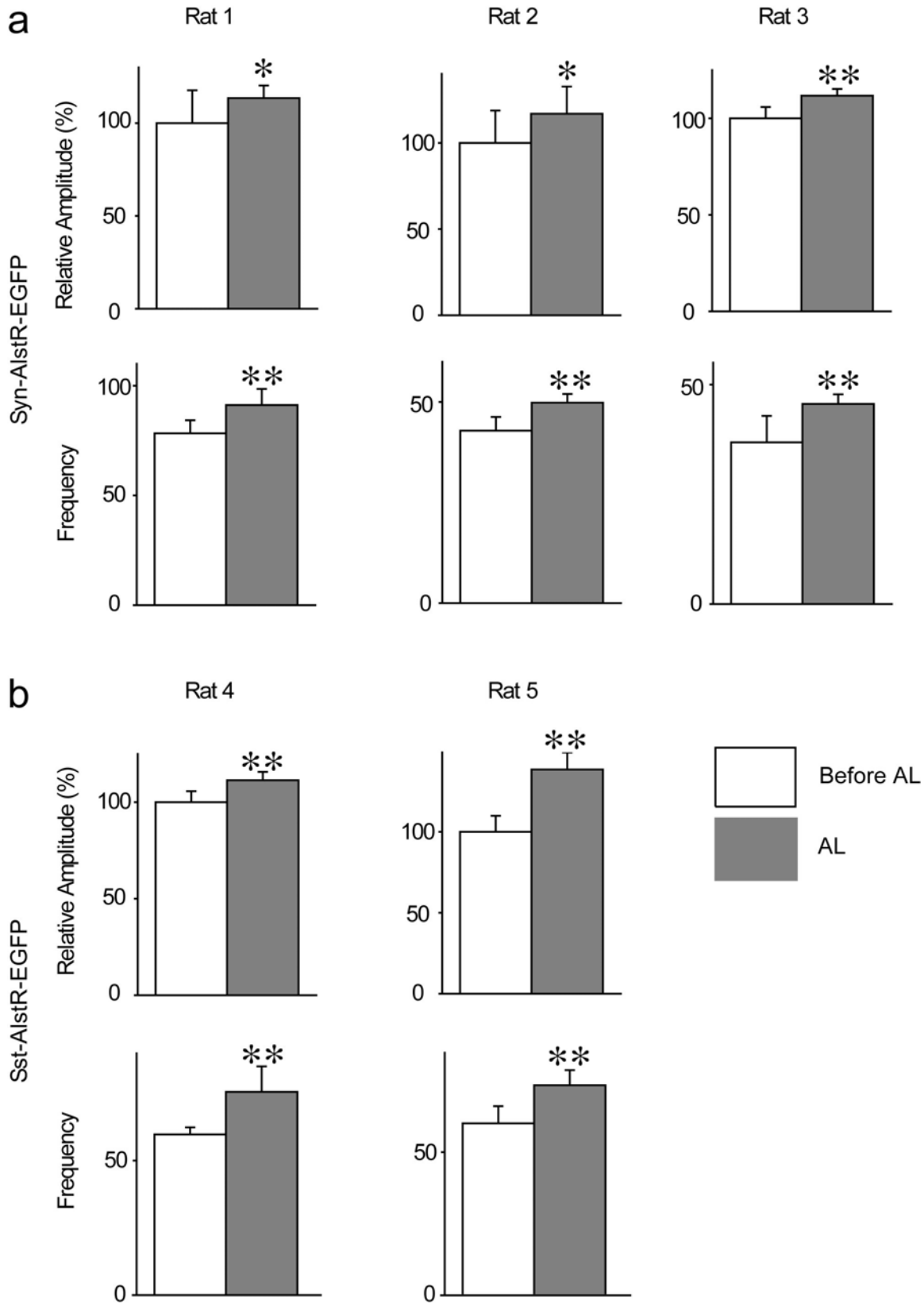
a
Rat 1
Rat 2
Rat 3
Syn-AlstR-EGFP
Relative Amplitude (%)
Frequency
100
50
0
*
**
b
Rat 4
Rat 5
Sst-AlstR-EGFP
Before AL
AL

Supplementary Figure 5 AL induced transient hyperventilation in some anesthetized rats injected with Syn-AlstR-EGFP or Sst-AlstR-EGFP AAV2. (**a**) Three Syn-AlstR-EGFP rats (1-3), and (**b**) two Sst-AlstR-EGFP rats (4-5) show significant increase of amplitude and frequency transiently within 20 seconds upon AL administration. Gray bars: Averages of normalized (to control) inspiratory amplitude and instantaneous frequency for all breaths 5-20 seconds after AL administration; White bars: Control averages of normalized inspiratory amplitude and frequency for all breaths 15 seconds prior to AL administration. 3 of 5 Syn-AlstR-EGFP (a) and 2 of 4 Sst-AlstR-EGFP (b) injected rats show the transient and significant increase of both amplitude ((a) and (b) upper panels) and frequency ((a) and (b) lower panels) after AL administration (*p<0.05, **p<0.0001, independent t-test). Values are mean±s.d.

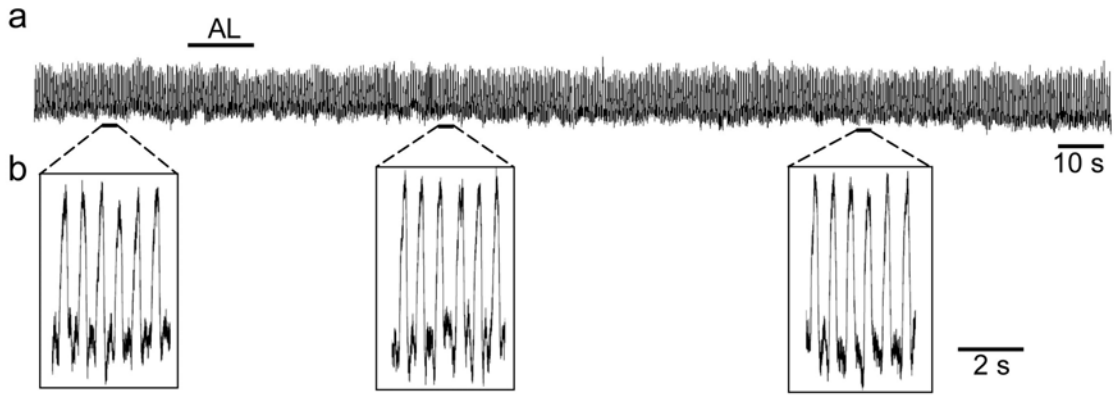

Supplementary Figure 6 Administration of AL *icc* does not affect the breathing patterns in control (uninfected) rats. (**a**) Plethysmographic record of breathing pattern after AL *icc* (0.42 μmole kg^{-1}). (**b**) Expanded sections from (a). Signal represents tidal volume.

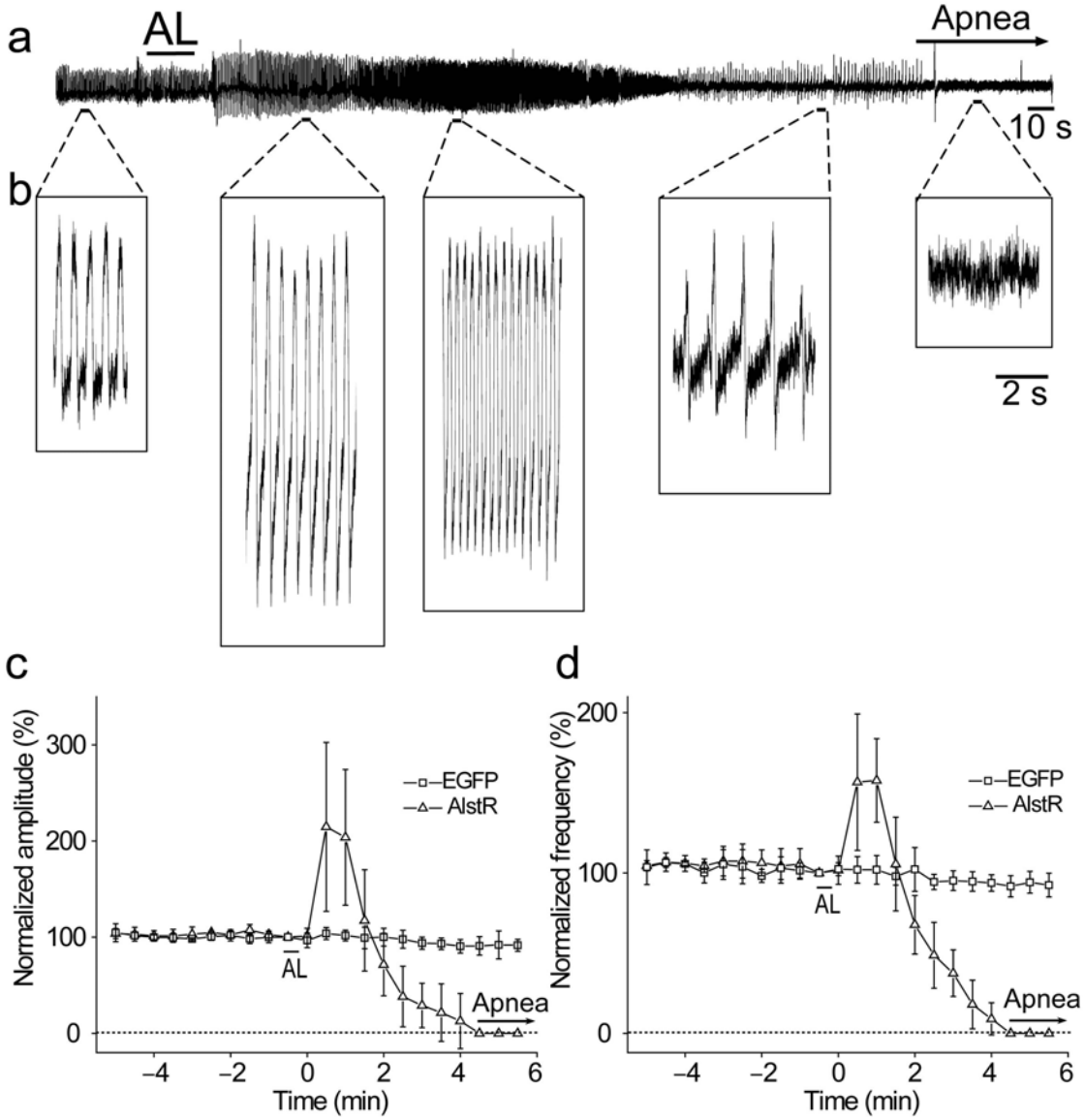

Supplementary Figure 7 Rapid silencing of preBötC AlstR-expressing neurons induces apnea in awake behaving rats. AL administered *icc* (0.42 μmole kg^{-1}) 4-6 weeks after bilateral preBötC microinjection of Syn-AlstR-EGFP. **(a)** Plethysmographic record of breathing pattern, signal represents tidal volume. **(b)** Expanded sections from (a). **(c), (d)** Changes of normalized frequency (c) and amplitude (d) upon AL application. Values are mean±s.d. (n=6).

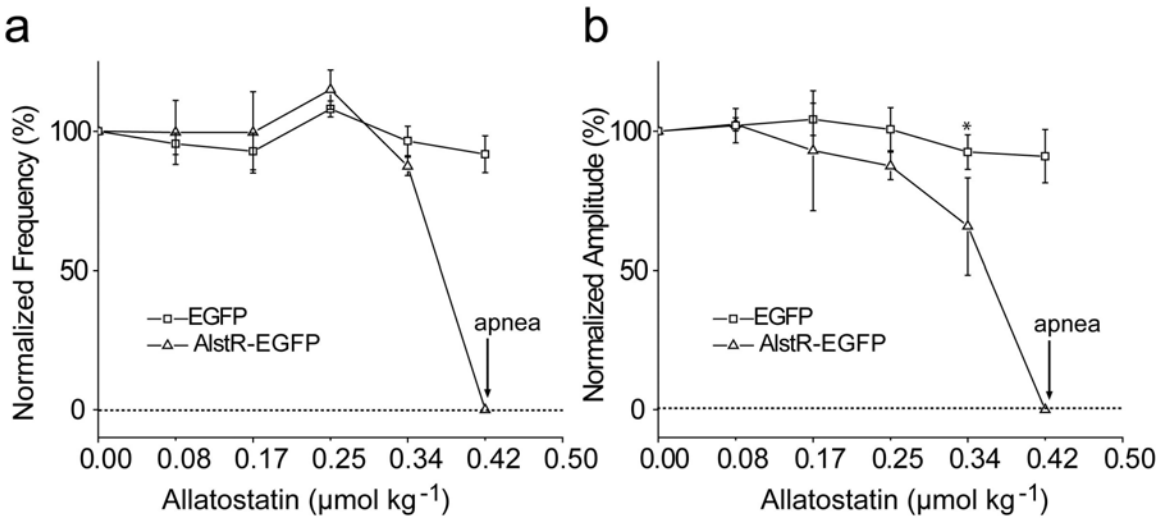

Supplementary Figure 8 Dose-response of AL. AL administered *icc* 4-6 weeks after bilateral preBötC microinjection of Syn-AlstR-EGFP or Syn-EGFP AAV2.
(**a**) Normalized frequency and (**b**) amplitude changes at 4.5 min after AL application in awake behaving rats. Values are means±s.d. of 6 rats * $p < 0.05$ (*t*-test).

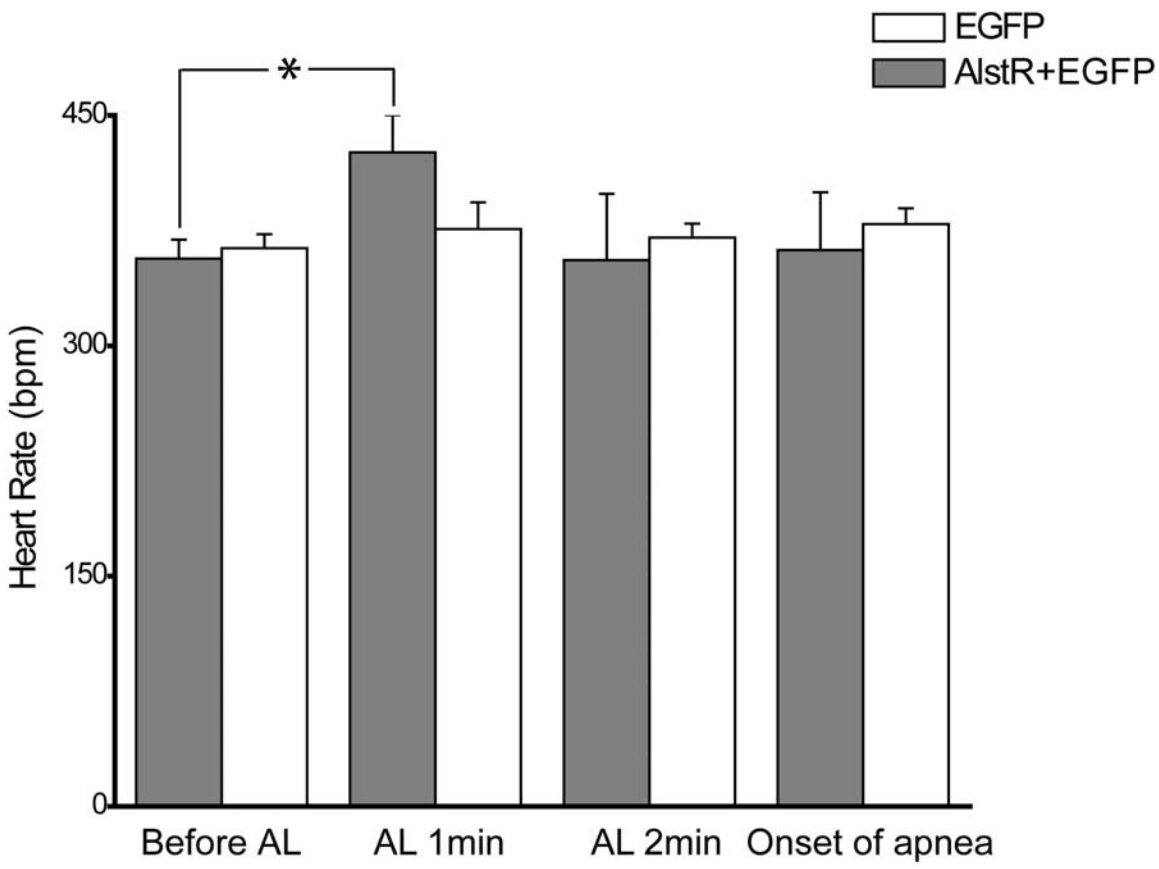

Supplementary Figure 9 Heart rate in awake rats was elevated during the early onset transient hyperventilation period but returned to control levels prior to the onset of apnea. Rats were injected with Syn-AlstR-EGFP. Heart rates (beat per minute, bpm) were determined by the EMG signal using Chart 5 software (AD Instruments, Colorado Springs, CO). Four time points were plotted: prior to AL administration: 357±12; AL 1 min: 426±24; 2 min: 356±43; and 4.5 min (onset of apnea) post AL application *(icc)*: 362 ±38; * $p<0.05$ (*t*-test). Values are means±s.d. of 3 rats.

Table 1. Absence of EGFP cell bodies in brainstem and spinal cord respiratory-related regions (except for the preBötC) after local viral injection.

	Syn promoter*	Sst promoter**
Periaqueductual grey	0	0
Parabrachial complex/ Kölliker Fuse	0	0
Parafacial respiratory group/Retrotrapezoid nucleus	0	0
Bötzinger complex	0~5&	0~5&
Hypoglossal nucleus/parahypoglossal region	0	0
Nucleus tractus solitarius	0	0
preBötzinger Complex	590±62	465±26
Ventral respiratory group caudal to preBötC	0	0
Ambiguus nucleus	0	0
Cervical motor neurons (C1-C4)	0	0

2 months post-viral injection, the cerebellum, brainstem, spinal cord and part of the midbrain was removed, sectioned, and EGFP was detected by immunohistochemistry. Every slice from -7.2mm from Bregma[21] to thoracic level of spinal cord was examined. We did not find any EGFP positive cell bodies beyond the preBötC injection sites. This data is consistent with numerous reports that AAV2 is not retrogradely transported[16-18].

&~0-5 EGFP positive cell bodies were found in the most caudal part of Bötzinger Complex, no EGFP positive cell bodies were found in rostral part of Bötzinger complex.

*Syn promoter AAV2: Syn-EGFP (n=3 rats), Syn-AlstR-EGFP (n=3 rats);

**Sst promoter AAV2: Sst-EGFP (n=6 rats), Sst-AlstR-EGFP (n=4 rats).

Table 2. Average number or percentage of preBötC neurons (within 250 μm from injection site) with phenotypic immunomarker (NeuN, Sst or NK1R) and coexpressing EGFP when expression was driven by synapsin vs. somatostatin promoter.

	Per side in preBötC		
	NeuN	**Sst**	**NK1R**
Average # neurons	2965	464	298
SYNAPSIN			
EGFP Neurons	590± 62 (n=7)	91±24 (n=3)	61±12 (n=9)
% Double positive of total phenotype	20±2% (n=7)	20±4% (n=3)	21±4% (n=9)
% Double positive of total EGFP	99±1% (n=7)	15±4% (n=3)	10±2% (n=9)
SOMATOSTATIN			
EGFP neurons	465±26 (n=6)	376±28 (n=4)	49±14(n=5)
% Double positive of total phenotype	16% (n=6)	81±8% (n=4)	16±5% (n=5)
% Double positive of total EGFP	100% (n=6)	80±6% (n=4)	11±3% (n=5)

Material and Methods

Adeno–associated viral vector construction and AAV2 preparation. AAV with an expression cassette of the synapsin promoter driving AlstR/EGFP, flanked by the AAV ITRs, was described previously[1]. The construct was named pA–Syn–AlstR–IRES–EGFP. The rat Sst promoter –750bp from transcriptional site is involved in cell specific expression, and contains the essential elements for basal and regulatory transcriptional activities[2,3]. We searched the homolog of this portion corresponding to the mouse Sst gene. Generally, longer distal promoter region renders more specific activity in Sst–expressing neurons, thus we cloned around 2.0kb of mouse Sst promoter region which contains the characterized region (–750bp) and 1.2kb more distal region of mouse Sst promoter. The mouse Sst promoter (2.0kb) was amplified by the primers (5' TTC GAA AGC CTA GAG GCA GAG CAA GCG CTG 3' and 5' TTC GAA GCT ATG GAG CTC TCC ACG GTC TCC 3' or 5' ACA TGT C GCT ATG GAG CTC TCC ACG GTC TCC 3'; the underlines indicate the BstBI and PciI sites respectively) from BAC RP23–274H19 and cloned into TOPO–T vector (Invitrogen), respectively. The Sst promoter fragments were cleaved by BstBI or BstBI plus PciI and inserted into BstBI site or BstBI plus NcoI sites of pA–Syn–AlstR–IRES–EGFP respectively to construct the pA–Sst–AlstR–IRES–EGFP or pA–Sst–EGFP. All the constructs were verified by sequencing.

AAV2 was prepared by using AAV Helper–Free System (Stratagene) according to the instructions of the manufacturer. Briefly, AAV2 was produced by transfection of AAV–293 cells in 150 mm dishes with 16 μg each of pAAV–RC, pHelper and a cloning viral vector generated above by using lipofectamine (Invitrogen). The cells were harvested at 72 hours post–transfection, lysed in 15 ml of gradient buffer (10 mM Tris (pH7.6), 150 mM NaCl, 10 mM $MgCl_2$) by four freeze/thaw cycles in dry ice–ethanol and 37°C bath, with addition of passing through a syringe with a 23G needle ten times. The lysate was treated by 50 U/ml of Benzonase (Sigma) for 30 min at 37°C, and clarified by centrifuge at 3,000 g for 15 min. The virus was purified by using iodixanol density gradient ultracentrifuge at 350,000 g for 1 hour at 18°C as described elsewhere[4]. The titer of the AAV2 was determined by quantitative PCR.

Surgical procedures. All experimental procedures were approved by the Chancellor's Animal Research Committee at the University of California, Los Angeles. The surgical procedures were described previously[5,6]. Briefly, male Sprague–Dawley rats (220 –250g) were anaesthetized with Ketamine (100 mg kg^{-1}) and Xylazine (10 mg kg^{-1}) injected intraperitoneally (i.p.). Rats breathed 1–1.5 vol% isoflurane in O_2 throughout the surgery. The skull was positioned in a stereotaxic apparatus with Bregma 5mm below Lambda. The dorsal medullary surface was exposed. Using a micropipette (40 μm tip diameter) guided by a micromanipulator, 0.5 μl of AAV2 virus (10^{10} particles ml^{-1}) in phosphate buffered saline (PBS) was injected into the preBötC at coordinates: 0.9 mm rostral, ±2 mm lateral and 2.7 mm ventral to the calamus scriptorius. In all rats, injections were made bilaterally. Microinjections were made at the rate of 0.2 μl min^{-1} using a series of pressure pulses (PicoSpritzer III, Parker Hannifin Corporation). The micropipette was left in place for 5 minutes post–injection to allow the viral solution to be absorbed and to minimize the backflow of the solution up the micropipette track. After microinjection, a catheter (0.6 mm diameter) was implanted into the cerebellomedullary cistern and fixed to the skull using bone cement. Pairs of biocompatible wire electrodes (Cooner Wire, Chatsworth, CA) were implanted for intercostal muscle electromyography and ECG measurement and tunneled subcutaneously to a socket secured to a skin button (Instech Laboratories, Inc., Plymouth Meeting, PA) implanted in between the shoulder blades. Muscles were sutured in layers using 6–0 absorbable sutures. Skin was sutured using 5–0 nylon. Sutures were removed 7 days post–surgery. After surgery, the rats were housed for 3–8 weeks to allow for expression of AlstR and EGFP.

Awake rats: Breathing was recorded using a whole body plethysmograph (Buxco Research Systems, Sharton, CT). The signal from the plethysmograph represents tidal volume. While in the plethysmograph, rats could move freely, with access to water and rat chow. Rats were studied for 4 hours in the plethysmograph for 8–12 times in between AAV2 injection and AL administration. AL was dissolved in saline to make the final concentration as 2 mM. At the end of a 4–hour recording session, AL (0.42 μmol kg^{-1}) was slowly (~30 sec.) injected via the implanted catheter (intracerebellomedullary cistern (*icc*)). The maximum dose was 0.16 μmole, even in rats that weighed >400 grams. Rats

were allowed to recover. In some rats, the procedure was repeated 3–4 weeks later, with similar results.

The initial response to AL administration in awake rats was a significant increase in ventilation. During this period rats stood "frozen" – a position associated with fear in rats, with an associated transient increase of heart rate that returned to control levels prior to the onset of apnea (Supplementary Figure 9). We speculate that this response was initiated by the mechanisms underlying the small but significant transient increase in ventilation seen in anesthetized rats, but manifested as a much larger response in the awake state. In humans complaining of dyspnea, a dissociation between metabolic needs and actual ventilation can lead to a sensation of discomfort. We suggest that this effect underlies the noticeable increase in ventilation in awake rats, but regardless of cause could not be sustained as preBötC neurons hyperpolarized.

During progressing hypoventilation and apnea, after a brief struggle, initially awake rats went passive, then limp. In initial experiments we were not able to rescue 5 awake rats whose apneas were 477, 215, 196, 170, or 162 seconds long; none of these rats gasped prior to death. One report[7] suggests the preBötC network underlies generation of multiple breathing patterns, including eupnea, sigh, and gasp. The lack of gasping is consistent with an essential role of the preBötC in gasping. In subsequent experiments all rats were rescued after 90 seconds of apnea. They were removed from the plethysmograph and connected to a ventilator *via* a sterile lubricated silicone tube inserted in one nostril. Rats are nose–breathers and their elongated soft palate facilitates effective ventilation via the nose. This mode of ventilation is comparable to mechanical ventilation using a nasal mask in humans. Ventilation continued until rats were able to breathe on their own (typically ~40 min. later). Rats were not restrained and free to remove the tube and detached themselves from the ventilator. Only two rats attempted to remove the nose tube after 20 min of ventilation. During prolonged ventilation these rats were in their natural (prone) position and were completely covered with a small towel.

Anesthetized rats: In anesthetized rats a tube was inserted in one nostril and connected to a flow head to continuously measure airflow. After rats were anesthetized, AL (0.42 μmol kg^{-1}) was slowly (~30 sec.) added *icc*. After 90 seconds of apnea, rats

were mechanically ventilated until they were able to breathe on their own, typically ~40–60 minutes.

Airflow and ECG signals were digitized and stored and analyzed using software from AD Instruments (Grand Junction, CO).

Rats were monitored for 1–12 weeks after AL administration. Their breathing was normal.

Immunohistochemistry. Rats were anesthetized with Nembutal (100 mg kg^{-1}, i.p.) and perfused transcardially with 4% paraformadehyde in PBS. The brainstem was removed and put in 4% paraformadehyde/PBS for another 2 hours, followed by cryoprotection overnight in 30% sucrose in PBS. Forty μm thick transverse sections were cut using a freezing microtome and incubated in primary antibodies, with 10% normal donkey serum for 24 or 48 hours at 4°C. The origins and dilutions of primary antibodies used in this study were: rabbit anti–Sst–14 (Pennisula Laboratories, LLC; 1:500 or 1:5000 for TSA see below); Alexa 488–conjugated rabbit anti–GFP (Molecular Probes, CA; 1:500); Chicken anti–GFP (Aves Labs, Inc., OR; 1:500); mouse anti–Neuronal Nuclei (NeuN) (Chemicon; 1:500); guinea pig polyclonal antibody to neurokinin–1 receptor (NK1R) (Biomol; 1:5000); rabbit anti–NK1R (Chemicon; 1:1000); and mouse anti–tyrosine hydroxylase (TH) (Chemicon; 1:500). Sst expression decreases with age[8,9]. We found significantly more Sst–ir neurons in preBötC in young compared to old rats. To facilitate detection of Sst positive neurons in older rats (>300grams) we used slightly different protocol. The animals were treated by 150μg colchicine in 50μl (*icc*) per rat for 24 hours before perfusion. The brainstems were fixed in 4% paraformadehyde/PBS at 4°C overnight after transcardial perfusion, followed by cryoprotection overnight in 30% sucrose in PBS; Rabbit anti–Sst–14 (1:5000) was incubated for 24 hours at 4°C and detected by using TSA/Tetramethyl–rhodamine system (Perkin Elmer, MA.). In some cases, guinea pig anti–NK1R polyclonal antibodies were used and signals were amplified by TSA system as well. Others primary antibodies were detected by rhodamine–conjugated donkey anti–rabbit secondary antibody (Jackson; 1:250); rhodamine–conjugated donkey anti–mouse secondary antibody (Jackson; 1:250); Alexa 488–

conjugated donkey anti–chicken secondary antibody (Jackson; 1:250); or FITC–conjugated donkey anti–rabbit secondary antibody (Jackson; 1:250).

Brainstem sections were grouped as one–in–four of sequential series of 40 μm transverse sections, thus four groups of brainstem sections were collected from each rat and immunohistochemistry was performed using the following four groups of primary antibodies: NK1R and EGFP, Sst and EGFP, NeuN and EGFP, and TH and EGFP. Images were acquired by confocal laser scanning microscope (LSM510 META, Carl Zeiss, Germany). High resolution Z–stack confocal images were taken at 0.45μm intervals. Confocal images were presented as Z–stack projections. Data measuring proportions of cells with EGFP colocalization with various other markers were obtained by counting the number of immunofluorescent–positive neurons within a 250 μm radius circle. This circle was positioned with the dorsal most point at the lower edge of the compact portion of the nucleus ambiguus.

Discussion

Specificity of AL: The inhibitory effects of AL on AlstR–expressing mammalian neurons *in vitro* and *in vivo* are well documented[1,10,11]: i) effects of AL are restricted to neurons expressing AlstR, and highly specific, and; ii) neurons expressing AlstR can be completely inactivated. Patch clamp recordings *in vitro* in AlstR–EGFP–transfected neurons demonstrate that neurons expressing EGFP are quickly hyperpolarized after administration of AL, whereas neurons that do not express EGFP remain unaffected. Here, we show that: i) in control rats (in which AlstR was not expressed) there was no response to AL (Fig 2, supplementary Fig 3, 4), and; ii) transfected neurons were found around the injection site in preBötC but not anywhere else (see Supplementary Table 1 and further comments below).

We have established that activation of AlstR on preBötC Sst neurons[12], presumably silencing them, leads to persistent apnea. The determination of the spatiotemporal details of the disturbances in preBötC circuits (and other connected populations, such as within the ventral respiratory column) will require electrophysiological recording.

Apnea was complete: After rats stopped breathing they were intubated through the nose and connected to an airflow head. Our flow measurements were so sensitive that in addition to flow resulting from contraction of the respiratory pump muscles, minute flow changes related to contraction of accessory respiratory muscles and heart beat could be detected. After administration of AL only flow changes related to the heart beat were observed, indicating inactivation of *all* respiratory muscles. The most parsimonious explanation for absence of respiratory activity in muscles supplied from variety of different motoneuronal pools is the loss of respiratory rhythm at its source.

Rhythmic expiratory muscle activity persists after inspiratory muscle activity is eliminated by silencing of preBötC neurons expressing the μ–opiate receptor (μOR) by means of systemic administration of μOR agonist–fentatnyl in neonatal and juvenile rats[13]. Here we report that after rapid hyperpolarization of preBötC Sst neurons all respiratory muscle activity, including that of the expiratory muscles, ceased. Why are these responses different? We suggest several possibilities. i) Expiratory oscillations may be inhibited by pontine neurons expressing μOR, and fentanyl lifts this inhibition[14]. Thus, fentanyl could promote rhythmic expiratory activity during inspiratory apnea in the adult rat; ii) In experiments with neonatal rats, they were kept hyperoxic. In contrast, in our experiments, rats became severely hypoxic, which inhibits expiratory oscillations; iii) Expiratory activity is robust in newborn and juvenile rats, but difficult to elicit in adults[15]; iv) The preBötC is the dominant oscillator in the adult; perhaps any second oscillator is incapable of independent oscillations in adult rats, and/or requires excitation from the preBötC in order to do so.

Localization of viral expression: In order to determine whether the virus was expressed distantly from the preBötC injection sites, e.g., due to long–distance diffusion or retrograde transport, we systematically looked for EGFP–positive cell bodies throughout the whole brainstem. Thus, all rats (n=24) infected with AAV2 were sacrificed and perfused; we cut sections (40 μm) from the medulla beginning at the level of the obex rostral through the caudal half of the facial nucleus. No EGFP–positive cell bodies were found outside of the region of the preBötC injection site, including in the nucleus tractus solitarius (NTS), and retrotrapezoid nucleus–parafacial respiratory group (RTN/pRFG).

In 16 of these virally injected rats, we also examined histological sections from the midbrain to the spinal cord including the cerebellum. In all cases, there was robust EGFP expression in the preBötC but we did not find *any* EGFP positive cell bodies beyond the injection sites (Supplementary Table 1). These results are consistent with numerous reports showing that AAV2 is not retrogradely transported[16–18]. Given the design of the viral vectors, EGFP is expressed wherever AlstR is expressed. Thus we conclude from the absence of EGFP outside the preBötC that there was no AlstR expression elsewhere except in EGFP–positive preBötC neurons, and all responses to AL were mediated by them. We also have another relevant observation. We injected the AAV2–EGFP virus into the hypoglossal nerve in 3 rats and into the genioglossus muscle in 3 rats, hoping to transfect motoneurons via axonal transport. No transfected motoneurons were found within the hypoglossal motor nucleus (data not shown).

Incidental damage to preBötC: In each experiment, we carefully examined the morphology of neurons and neuronal numbers in and around the preBötC after immunostaining. We did not find scar tissue, or obvious damage, such as gliosis, nor did we observe quantitative changes in total neurons, NK1R neurons, TH neurons and Sst neurons in the preBötC (Supplementary Table 2) after months of viral expression, which suggest there was no cytotoxicity or inflammation. At a behavioral level, infected rats gained weight, breathed and moved normally, etc. Rats were still healthy five months after initial surgery (n=8). These observations are in contrast to the long–term effects of injection of Substance P–saporin into the preBötC[5], where we readily observed proliferation of glia at the injection site. The AAV2 virus does not seem to trigger any immune reaction in the preBötC in adult rats, consistent with many reports showing that AAV2 causes very little cytotoxicity or inflammation[1,19].

Rates of viral expression and differences in responses to AL between viruses with Syn or Sst promoters: After transfection, AAV2 DNA integrates with the neuronal genome, thus protein expression becomes constitutive, and the expression rate depends on the promoter activity. The onset of detectable EGFP signal is ~2 weeks postinjection in Syn–EGFP injected rats, and ~3 weeks postinjection in Sst–EGFP injected rats (data not shown).

Thus, the Sst promoter activity can be considered weaker than the Syn promoter in preBötC neurons. EGFP expression is weaker under IRES in Syn (or Sst) –AlstR–EGFP than under Syn (or Sst) promoter in Syn (or Sst)–EGFP. Thus, it will take more time to have equivalent levels of EGFP signal in AlstR–EGFP viruses (4 weeks for Syn promoter and 6 weeks for Sst promoter) than EGFP control viruses. Efficient AlstR expression in preBötC is necessary in order to elicit a response by AL in awake rats. Apnea could be successfully induced by application of AL at 4 weeks post–injection of Syn–AlstR–EGFP or 6 weeks post–injection of Sst–AsltR–EGFP, which is consistent with timing of EGFP expression by these viruses. Moreover, the onset of apnea following AL administration was sooner in rats transfected with viruses carrying the Syn promoter compared to the Sst promoter. There are several additional possible explanations for these differences: i) more neurons were transfected by Syn compared to Sst (Table 2); ii) Syn transfected another phenotype of preBötC neuron that when silenced had a more powerful effect on breathing compared to preBötC Sst neurons, and; iii) more AlstRs were expressed per neuron by the Syn promoter compared to the Sst promoter resulting in more rapid silencing in the former case. Further investigation will be required to distinguish among these possibilities, including identification of the neuronal phenotypes and AlstR expression rates among subpopulations transfected by the AAV2 viruses and electrophysiological recording of the activity of preBötC neurons before and after AL administration.

Differences in responses to AL between anesthetized and awake rats: Our results show that the time profiles of the perturbations of inspiratory amplitude and frequency in the anesthetized versus awake animals differ. Anesthesia does (at least) two things of relevance: i) by depressing consciousness, anesthesia depresses volitional/emotional responses to changes in ventilation such as might be associated with anxiety or panic in response to dyspnea, and; ii) depresses neuronal excitability, e.g., by potentiating GABAergic neurotransmission or inhibition of NMDA receptors. preBötC neurons are most proximal to the ventral medullary surface (preBötC neuronal somas are 150–700 μm to the ventral surface in adult rats), with dendrites extending to the ventral, but not dorsal surface, of the medulla. As AL diffuses from the CSF into the brainstem it would affect the distal, then proximal, dendrites, then somas of transfected preBötC neurons.

We suggest two possibilities: initial activation of dendritic AlstRs induced ectopic currents in preBötC neurons, paradoxically exciting them prior to their ultimate depression, and/or; AL induced synchronous opening of K^+ channels that led to extracellular accumulation of K^+ in the vicinity of transfected neurons that depolarized adjacent preBötC neurons to transiently increase respiratory rate. Respiratory–modulated oscillations of K^+ as large as 1.3–1.5 mM are seen in the vicinity of respiratory neurons in the cat[20]. In some anesthetized rats (3 out of 5 Syn–AlstR–EGFP, and 2 out of 4 Sst–AlstR–EGFP), there was a transient, slight but significant increase of amplitude and frequency with 20 seconds upon AL administration (Supplementary Fig. 5), though group data did not reach statistical significance. These results show transient hyperventilation upon AL administration in both anesthetized and awake animals.

*Differences between slow lesions and rapid silencing of preBötC neurons:*When substance P –Saporin is used to lesion preBötC NK1R neurons in adult rats, the breakdown in normal breathing occurs over ~1 week[5,6], giving sufficient time for compensatory mechanisms to act to ultimately produce a (pathological) rhythm, i.e., no persistent apnea, during wakefulness. In contrast, in rats expressing AlstR, the silencing of preBötC neurons following AL administration occurred within minutes and resulted in a persistent apnea that would not recover before asphyxiation. Our results suggest that compensatory mechanisms cannot act rapidly enough when the depression of preBötC neuronal excitability is sudden, which may provide insight into mechanisms of catastrophic respiratory failure in some cases of sudden infant death syndrome or sudden infant unexplained death, and central sleep apnea.

References for Supporting Online Material:

1. Tan, E.M. *et al. Neuron* **51**, 157–170 (2006).
2. Andrisani, O.M., Hayes, T.E., Roos, B. & Dixon, J.E. *Nucleic Acids Res* **15**, 5715–5728 (1987).
3. Patel, Y.C. *Front Neuroendocrinol* **20**, 157–198 (1999).
4. Zolotukhin, S. *et al. Gene Ther* **6**, 973–985 (1999).
5. Gray, P.A., Janczewski, W.A., Mellen, N., McCrimmon, D.R. & Feldman, J.L. *Nat Neurosci* **4**, 927–930 (2001).
6. McKay, L.C., Janczewski, W.A. & Feldman, J.L. *Nat Neurosci* **8**, 1142–1144 (2005).
7. Lieske, S.P., Thoby–Brisson, M., Telgkamp, P. & Ramirez, J.M. *Nat Neurosci* **3**, 600–607 (2000).
8. Hayashi, M., Yamashita, A. & Shimizu, K. *Brain Res* **749**, 283–289 (1997).
9. Lu, T. *et al. Nature* **429**, 883–891 (2004).
10. Gosgnach, S. *et al. Nature* **440**, 215–219 (2006).
11. Lechner, H.A., Lein, E.S. & Callaway, E.M. *J Neurosci* **22**, 5287–5290 (2002).
12. Stornetta, R.L. *et al. J Comp Neurol* **455**, 499–512 (2003).
13. Janczewski, W.A. & Feldman, J.L. *J Physiol* **570**, 407–420 (2006).
14. Onimaru, H., Kumagawa, Y. & Homma, I. *J Neurophysiol* **96**, 55–61 (2006).
15. Pagliardini, S., Janczewski, W.A. & Feldman, J.L. *37th annual meeting of the Society of Neuroscience (San Diego, CA, USA, 2007).*
16. Chamberlin, N.L., Du, B., de Lacalle, S. & Saper, C.B. *Brain Res* **793**, 169–175 (1998).
17. Davidson, B.L. *et al. Proc Natl Acad Sci U S A* **97**, 3428–3432 (2000).
18. Klein, R.L. *et al. Exp Neurol* **150**, 183–194 (1998).
19. Tenenbaum, L. *et al. J Gene Med* **6 Suppl 1**, S212–222 (2004).
20. Richter, D.W., Camerer, H. & Sonnhof, U. *Pflugers Arch* **376**, 139–149 (1978).
21. Paxinos, G. & Watson, C. 4 ed.; Academic Press.: San Diego, CA (1998).